Connecting the Reentrant Insulating Phase and the Zero-Field Metal-Insulator Transition in a 2D Hole System

R. L. J. Qiu,[1] X. P. A. Gao,[1,*] L. N. Pfeiffer,[2] and K. W. West[2]

[1]*Department of Physics, Case Western Reserve University, Cleveland, Ohio 44106, USA*

[2]*Department of Electrical Engineering, Princeton University, Princeton, New Jersey 08544, USA*

(Received 21 September 2011; published 7 March 2012)

We present the transport and capacitance measurements of 10 nm wide GaAs quantum wells with hole densities around the critical point of the 2D metal-insulator transition (critical density p_c down to $0.8 \times 10^{10}/\mathrm{cm}^2$, $r_s \sim 36$). For metallic hole density $p_c < p < p_c + 0.15 \times 10^{10}/\mathrm{cm}^2$, a reentrant insulating phase (RIP) is observed between the $\nu = 1$ quantum Hall state and the zero-field metallic state and it is attributed to the formation of pinned Wigner crystal. Through studying the evolution of the RIP versus 2D hole density, we show that the RIP is incompressible and continuously connected to the zero-field insulator, suggesting a similar origin for these two phases.

DOI: 10.1103/PhysRevLett.108.106404 PACS numbers: 71.30.+h, 73.40.−c, 73.63.Hs

Strongly correlated electron systems have offered numerous interesting topics for mankind to explore, e.g., Fermi liquid, Wigner crystal (WC), fractional quantum Hall (QH) effect [1], and high-temperature superconductivity [2]. In the two-dimensional (2D) case, a possible phase transition between metal and insulator, which contradicts the scaling theory of localization for noninteracting 2D fermions [3], was discovered by Kravchenko *et al.* [4]. The origin of this metal-insulator transition (MIT) in strongly correlated 2D electron or hole systems has been of great interest [5,6]. A relevant question is how the zero-field ($B = 0$) MIT is related to the 2D QH states. In early experiments, the phase diagram maps against 2D carrier density p and perpendicular magnetic field B obtained from the transport [7] and thermodynamic compressibility data [8] suggested that B transforms the $B = 0$ insulator into the QH liquid, somewhat similar to the conventional Anderson insulator-QH transition [9]. Besides the zero-field MIT and $B = 0$ insulator to $\nu = 1$ QH transition, 2D electron or hole systems are known to exhibit rich transitions between the so-called high field insulating phases (HFIPs) [10], reentrant insulating phases (RIPs) [11–14], and the fractional QH states at high magnetic fields where the Landau-level filling factor $\nu < 1$. All the HFIPs and RIPs among fractional QH states in GaAs/AlGaAs systems are widely believed to be caused by the forming or melting of WC [11–18] due to the strong Coulomb interaction. Moreover, the observations of pinning mode of the WC oscillating in the disorder potential in microwave transmission experiments [19–22] offer more direct evidence for the WC interpretation.

On the theory side, quantum Monte Carlo calculations [23–26] had located that the liquid-WC transition should happen around a critical value of $r_s \sim 37$ at $B = 0$ ($r_s \equiv 1/[a_B^* \sqrt{\pi p}]$, is the ratio between the typical potential and kinetic energies, where $a_B^* = \hbar^2 \epsilon / m^* e^2$ is the effective Bohr radius). At $B > 0$, the simulations by Zhu and Louie [26] even determined that the phase boundary starts from $\nu \sim 1/6.5$ and moves to higher ν when r_s increases (density decreases). The results, together with other variational studies [27], supported the interpretation of the observed HFIPs and RIPs as pinned WCs. However, the liquid-WC transition phase diagram remains unsettled [28,29], especially in the range from $\nu = 1$ to the $B = 0$ limit, since a reentrant WC that was expected at $\nu > 1$ (Ref. [26(b)]) has never been observed experimentally. Therefore, the relation between those HFIPs, RIPs and zero-field insulating phase in 2D systems with large r_s is still unclear.

In this Letter, we report the first experimental evidence connecting the zero-field insulating phase of the 2D MIT to the RIP in finite B via the observation and systematic study of a new RIP between the $\nu = 1$ QH state and the $B = 0$ MIT in a dilute 2D hole system (2DHS) in GaAs. We suggest that this RIP is a pinned WC since it is incompressible [8,30] and its peak resistance $R_{\mathrm{RIP}} \propto \exp(\Delta_{\mathrm{RIP}}/2T)$ (Δ_{RIP} up to 0.52 K at $p = 0.55 \times 10^{10}/\mathrm{cm}^2$ for our highest mobility sample), resembling the previously observed low ν RIPs in GaAs dilute 2D electron [11,12] or hole [13,14,17] systems. Our transport and compressibility phase diagrams indicate a unified phase boundary linking zero-field MIT with the RIP between the $\nu = 1$ and $\nu = 2$ QH states and the HFIP, consistent with the qualitative phase diagram proposed by Ref. [26(b)]. The results presented here suggest that the zero-field MIT is a liquid-WC transition.

Our transport measurements were performed down to temperature $T = 50$ mK on four high mobility 10 nm wide p-type GaAs quantum-well (QW) samples (5A, 5B, 11C, and 11D) with low 2D hole density. Thermodynamic compressibility measurement was done on QW 11D by measuring the capacitance between the 2D channel and top gate. All of the four GaAs QWs are similar to those used in our previous studies [31–34], which were grown on (311)A

GaAs wafer using $Al_{0.1}Ga_{0.9}As$ barriers and Si delta-doping layers placed symmetrically at a distance of 195 nm away from the 10 nm QW. QW 5A and 5B were taken from wafer 5-24-01.1, and sample 11C and 11D were taken from another wafer 11-29-10.1. All the samples have density $p \sim 1.3$ (the unit for p is $10^{10}/\mathrm{cm}^2$ throughout this Letter) from doping. Without gating, QW 5A and 5B have a mobility $\simeq 5 \times 10^5$ $\mathrm{cm}^2/\mathrm{V\,s}$, while QW 11C and 11D's mobility $\simeq 2 \times 10^5$ $\mathrm{cm}^2/\mathrm{V\,s}$. The back gates used to tune the hole density are approximately 150 μm away from the well for QW 5A and 5B (300 μm spacing for 11C), to avoid the screening of the Coulomb interaction between holes by the back gate. Samples 5A and 5B were fabricated into Hall bars with approximate dimensions 2.5 mm $\times$ 9 mm for 5A and 2 mm $\times$ 6 mm for 5B, and six diffused In(1%Zn) contacts; sample 11C is a square one (5 mm $\times$ 5 mm) with diffused In(1%Zn) contacts in Van de Pauw configuration. The measurement current was along the high mobility [$\bar{2}33$] direction and stayed low so the heating power is less than 3 $\mathrm{fW}/\mathrm{cm}^2$ to prevent overheating the holes [35]. The compressibility measurement sample QW 11D has a size of 4.5 mm $\times$ 5 mm, with four diffused In (1%Zn) contacts in Van de Pauw configuration and coated with Ti/Au top gate, which is 400 nm away from the well. Capacitance was measured by applying a low frequency (f = 3–13 Hz) excitation voltage V_{ex} (typically 200 μV) to the top gate and monitoring the 90° out of phase current I_y, obtaining the capacitance $C = I_y/2\pi f V_{\mathrm{ex}}$. A dc voltage V_g was superimposed to tune the density via top gate. The measured capacitance can be viewed as two capacitors in series: $1/C = 1/C_0 + 1/C_q$, where C_0 is geometric parallel plate capacitance between the top gate and the 2DHS, and C_q is the quantum capacitance of charging the 2DHS. The quantum capacitance C_q is proportional to the compressibility κ: $C_q = e^2 dp/d\mu = e^2 p^2 \kappa$ (here μ is the chemical potential, $dp/d\mu$ is the thermodynamic density of states).

Figure 1 is shown to establish the existence of MIT and reentrant insulating behavior at $\nu > 1$ in our low-density 2DHS. With the tuning of the back gate [36], we were able to do transport measurement in a density range of 0.45–2.2, corresponding to $r_s \sim 22$–48 (using effective hole mass $m^* = 0.3m_e$ [37]). Figure 1(a) presents the temperature dependence of the longitudinal resistivity of sample 5B, demonstrates a MIT at $B = 0$, with a critical density $p_c \approx 0.8$ ($r_s \approx 36$). Similar data and critical density were obtained on sample 5A. The critical point of MIT for samples 11C and 11D is around $p_c = 0.95$ ($r_s \approx 33$), due to the slightly lower mobility of the wafer. All the p_c values are lower than the critical density in Refs. [7–9,38], reflecting the better sample quality in this study.

The 2D hole density is determined by the dip positions of the Shubnikov–de Haas (SdH) oscillations as $p = \nu B_\nu e/h$, where B_ν is the perpendicular magnetic field at the corresponding Landau filling factor ν. In Fig. 1(b), the

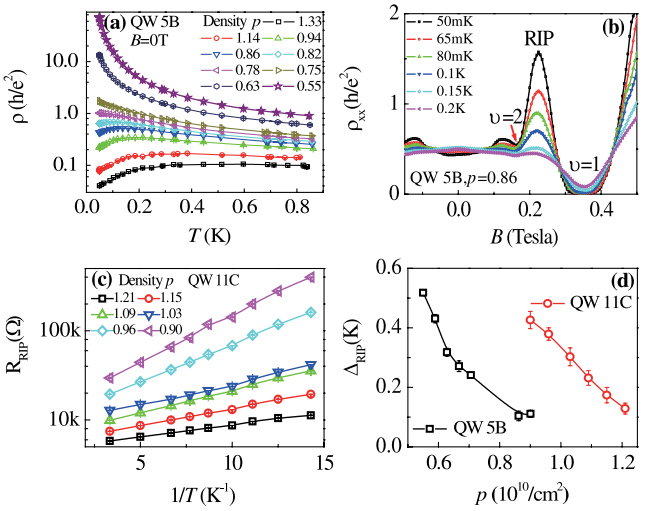

FIG. 1 (color online). (a) Zero-field MIT with a critical density $p_c \sim 0.8 \times 10^{10}/\mathrm{cm}^2$ in a 10 nm wide GaAs QW (sample 5B); $\rho(T)$ at p = 1.33, 1.14, 0.94, 0.86, 0.82, 0.78, 0.75, 0.63, 0.55 are shown. (b) Magnetoresistivity of sample 5B with $p = 0.86$ at T = 50 mK, 65 mK, 80 mK, 0.1 K, 0.15 K, and 0.2 K. The reentrant insulating phase (RIP) resides between the $\nu = 1$ and $\nu = 2$ QH states. (c) Arrhenius plot of the resistance at the peak of the RIP from sample 11C ($p_c \sim 0.95 \times 10^{10}/\mathrm{cm}^2$) at densities of 0.9, 0.96, 1.03, 1.09, 1.15, and 1.21.(d) Fitted thermal activation gap Δ_{RIP} vs hole densities in samples 5B and 11C.

longitudinal magnetoresistivity $\rho_{xx}(B)$ for $p = 0.86$ of sample QW 5B is shown at various T from 50 mK to 0.2 K. At small magnetic fields, the sample exhibits metallic behavior. However, it is striking to see an unexpected insulating peak below 150 mK between the $\nu = 1$ and the $\nu = 2$ quantum Hall resistivity dips. This RIP is observed in all of our four 10 nm QWs. Another example of the RIP between $\nu = 1$ and $\nu = 2$ QH states can be seen in Fig. 1(c) of our previous paper [34]. As shown in Fig. 1(c) here, the resistance at the peak of the RIP follows exponentially activated T dependence and greatly exceeds the zero-field resistivity for the same density. Apparently the T dependence of the insulating peak is far stronger than that of the ordinary SdH oscillation amplitude, which is determined by the thermal damping factor, $X_T/\sinh(X_T)$, where $X_T = 2\pi^2 k_B T/\hbar\omega$. As another example, the peak resistivity for sample QW 5A exceeds the value of 12 K Ω/square, 6 times larger than ρ at $B = 0$, at T = 18 mK and $p = 1.13$ (Ref. [34]). Figure 1(c) illustrates the T-dependent resistance of QW 11C at the peak of RIP for densities from $p = 1.21$ to 0.9 in an Arrhenius plot. Similar to the RIPs between fractional QH states in GaAs/AlGaAs 2D electron [11] or hole [13,17] systems, the R_{RIP} vs T of QW 5B and QW 11C is exponential, $R_{\mathrm{RIP}} \propto \exp(\Delta_{\mathrm{RIP}}/2T)$. The fittings according to the thermal activation model give activation gaps Δ_{RIP} up to 0.52 K, shown in Fig. 1(d) for QW 5B and QW 11C. For both QWs, the value of Δ_{RIP} increases rapidly as the density decreases. Besides, the insulating phase emerges at higher density in

the lower mobility samples (QW 11C and 11D) than higher mobility samples (QW 5A and 5B), suggesting that disorder also tends to increase the stability of this RIP. The Hall resistance data [34,36] indicate that the $\nu = 1$ QH state is well formed but Hall resistance is suppressed significantly ($\sim$ 20%–30%) compared to the classical value $1/pe$ at the RIP and lower magnetic fields.

The similarity in the transport properties between the observed insulating phase at $\nu > 1$ and the previously studied RIPs between fractional QH states at $\nu < 1$ suggests that the insulating phase observed here is the RIP at $\nu > 1$ in the phase diagram proposed by Zhu and Louie (Fig. 14 in Ref. [26(b)]). Moreover, we performed capacitance measurements to elucidate the thermodynamic compressibility of the RIP observed here. Our experiment indicates that this RIP is more incompressible than both the $\nu = 1$ QH state and the $B = 0$ state, offering further evidence supporting the pinned Wigner crystal as the interpretation according to the phase diagram in Ref. [26(b)]. Figure 2(a) presents the magnetic-field-dependent top gate capacitance (symbol) $C(B)$ for several densities ($p = 1.73$, 1.42, 1.25, 1.12, 1.02, 0.95, 0.86) in QW 11D at 70 mK, together with the corresponding magnetoresistance curves (solid lines). In the lower three panels where $p > 1.2$, the capacitance value drops strongly at the $\nu = 1$ QH state, reflecting the 2D system's small thermodynamic density of states (compressibility) when the Fermi level resides in the Landau-level energy gap at low T. At low magnetic fields, the gate capacitance remains constant around the geometric capacitance value [marked as dashed horizontal lines in Fig. 2(a)] due to the fact that quantum capacitance C_q of 2D systems is very large and does not contribute much in the measured capacitance until strong Coulomb interactions reduces the compressibility significantly in the low-density regime. What is most interesting in Fig. 2 is, however, the behavior of capacitance as 2D hole density p decreases towards the critical density ($p_c \sim 0.95$). As Fig. 2(a) shows, the capacitance dip at $\nu = 1$ weakens as density decreases (dotted gray arrow). But a new dip in the capacitance vs B curve emerges at the position where transport data show the reentrant insulating behavior (light gray arrow). It is remarkable to note that the compressibility of the RIP is not only smaller than the zero-field state, but also the $\nu = 1$ QH state. Moreover, since capacitance values smaller than the geometric value were observed, the sign of the compressibility for the RIP is positive, in contrast to the well-known negative compressibility of 2D electron liquids. In addition to the capacitance dip at the RIP between $\nu = 1$ and 2, the sample's capacitance also drops at $\nu < 1$, corresponding to the HFIP.

Previously, it is known that the 2D system's compressibility approaches zero in the insulating phase of MIT [8]. This behavior is also observed in our sample, as shown by the reduced capacitance value of our sample at $B = 0$ when the carrier density is decreased to below $p_c \sim 0.95$ [top two panels in Fig. 2(a)]. But for hole densities around the critical density, the application of perpendicular magnetic field induces the RIP with more strongly insulating transport behavior as well as lower capacitance (compressibility) than the zero-field state. This observation motivates us to explore the relation between the RIP and the zero-field insulating phase of 2D MIT. We examine the 2DHS's phase diagram against p and B by both transport and capacitance measurements. Figures 2(b) and 2(c) plot the colored contour maps of longitudinal resistance and capacitance for QW 11C and QW 11D from 0 T up to 0.8 T over the density range $0.8 < p < 1.5$ at 70 mK. In Fig. 2(b), the three red finger-shaped areas pointing towards origin are the $\nu = 1$, 2, and 3 QH states. Similarly, the violet finger in Fig. 2(c) represents $\nu = 1$ QH state. Because of the dominance of

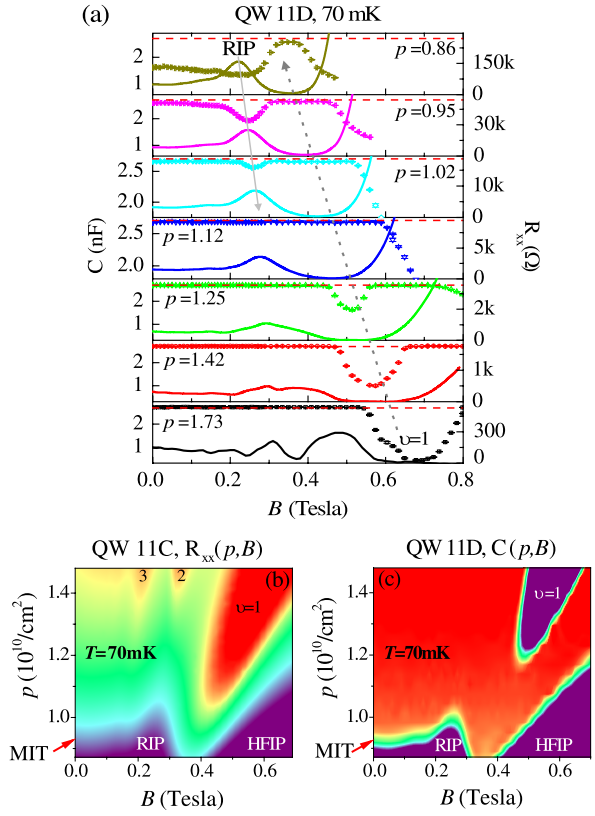

FIG. 2 (color online). (a) Capacitance (symbol) and resistance (line) vs perpendicular magnetic field for QW 11D at 70 mK at $p = 0.86$, 0.95, 1.02, 1.12, 1.25, 1.42, and 1.73. The $\nu = 1$ QH state gradually weakens as the density decreases, and eventually disappears, followed by the emergence of the new RIP. The dashed line is the estimated value of geometric capacitance C_0.(b) Longitudinal resistance map of QW 11C in p-B plane at 70 mK. As the color varies from red (in the $\nu = 1$ QH) to violet (in the RIP or HFIP), the resistance increases from $\leq$ 300 Ω to $\geq$ 300 kΩ in a log scale. The area with resistance larger than 300 kΩ is filled with violet. (c) Capacitance of QW 11D in p-B plane at 70 mK. The capacitance drops from 2.7 to $\leq$ 2.2 nF as the color changes from red (in the area between the $\nu = 1$ QH and the RIP or HFIP) to violet (in the $\nu = 1$ QH and RIP or HFIP).

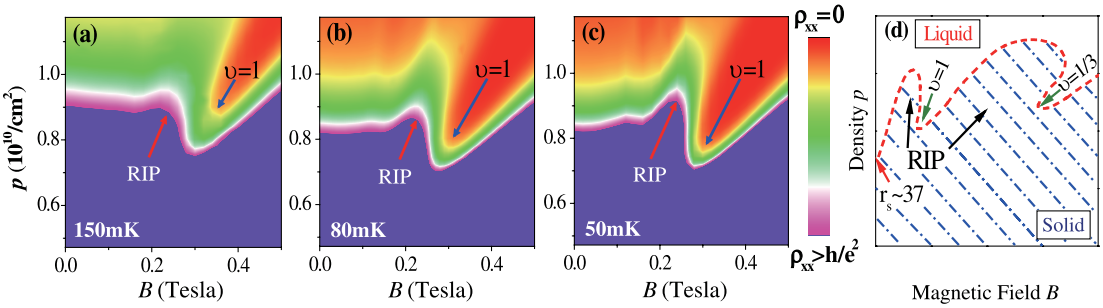

FIG. 3 (color online). (a),(b),(c) Contour map of the longitudinal resistivity of a 10 nm wide p-type GaAs QW (sample QW 5B) in the p-B plane at $T = 150$, 80, and 50 mK. (d) Schematic phase diagram converted from Fig. 14 of Ref. [26(b)], in which the Wigner solid phase is predicted to exist between the 2D hole liquid at $B = 0$ and the QH liquids at $\nu = 1$ and $1/3$.

C_0 in measured C, the $\nu = 2$ and 3 QH states were not resolved in our capacitance data. In Fig. 2(b) of transport map, the insulating phase is shown in violet at the bottom, which also has low capacitance (compressibility) as seen in Fig. 2(c). Through comparing the two maps, it is significant to see a unified phase boundary linking the zero-field MIT with the new RIP and HFIP in both transport and compressibility data. This connection between the zero-field insulator and the new RIP suggests a common origin for these two phases. It is necessary to point out that our phase diagram differs from previous study [7] in that there is a RIP protruding into the high density metallic regime while previous finding in higher density samples showed a phase boundary line moving down monotonically as B increases towards the $\nu = 1$ QH [7]. Our phase boundary coincides with the phase diagram in Fig. 14 of Ref. [26(b)], which predicts an insulating solid phase between the $B = 0$ liquid state and the $\nu = 1$ QH state [see Fig. 3(d)].

We also studied the temperature evolution of the phase boundary of the MIT in the p-B map via transport measurement. Figure 3 shows the longitudinal resistance maps of QW 5B for $B = 0$–0.5 T and $0.5 < p < 1.2$ at $T = 150$, 80, and 50 mK. This evolution depicts an interesting competition between the zero-field MIT and the formation of integer QH and the RIP. First, as T decreases, both the low field metallic state and the $\nu = 1$ QH become better formed as shown by the growing low resistivity (red) areas in the phase diagram towards lower density. At the same time, the RIP starts to form and protrude towards higher density in the diagram. Naturally, the implication is that the new RIP and the $\nu = 1$ QH state are the ground states in the $T = 0$ K limit. We point out that our observed RIP protruding into the $B = 0$ metallic liquid and the $\nu = 1$ QH liquid in the phase diagram is in agreement with the generic phase boundary predicted in Ref. [26(b)] where the WC "penetrates" into the 2D hole liquid phases between $B = 0$ and $\nu = 1$, as shown in the low field regime of the schematic phase diagram in Fig. 3(d). Interestingly, the theoretical phase diagram also predicts that the WC would make transition to $\nu = 1/3$ fractional QH liquid at higher B and p. Further experiments are under way to explore that part of the phase diagram in our dilute 2DHS. We also note that in Figs. 3(a)–3(c), all values of $\rho > h/e^2$ are assigned by a single color to highlight the qualitative consistency between data and the shape of the theoretical phase boundary in Ref. [26(b)]. The transition between RIP and the liquid phase at $B = 0$ or $\nu = 1$ appears to be not very abrupt, as seen in the resistivity data plotted over broader range in Figs. 1(b), 2(a), and 2(b). This might be related to the theoretical proposal that the electron liquid to WC transition is not a first order transition but a Coulomb frustrated continuous transition [39].

The phase diagram of our narrow QWs is distinct from those of wide QWs or heterostructures [7,8,17]. The RIP between the $\nu = 1$ and $\nu = 2$ QH states in strongly interacting 2D systems, even proposed decades ago [26], has never been reported in the literature. We believe that the narrow QW width is a key in the formation of this RIP at $\nu > 1$. Empirically, it has already been noticed that the RIP in the GaAs 2D electron system shifts to a higher filling factor as the QW width decreases [40]. Another argument is in the GaAs hole system, Landau-level mixing is significant and the well width will affect the hole effective mass, which is essential to the Monte Carlo calculation [26]. Furthermore, spin polarization was seen to induce a more dramatic effect in driving the metallic state into the insulating phase in a narrow QW system [33]. Therefore, the strong spin polarization close to the $\nu = 1$ QH state may have also helped the formation of the RIP.

In summary, we have observed a new RIP between the $\nu = 1$ and $\nu = 2$ QH states in a dilute p-GaAs system with narrow QW width. Our result suggests that this RIP is connected with the zero-field insulating phase of the 2D MIT. The RIP is similar to those observed at $\nu < 1$ among the fractional QH states in other GaAs heterostructures or QWs with wider width. Based on transport and thermodynamic compressibility experiments, we propose its origin to be related to the formation of disorder pinned WC. Both our transport and thermodynamic phase diagrams match the liquid-WC phase diagram proposed by Zhu and Louie [26], leading to the suggestion that the zero-field MIT is a liquid-WC transition [5,39,41].

X. P. A. G. thanks S. Kivelson for useful discussion. The authors thank the NSF for funding support (DMR-0906415). The work at Princeton was partially funded by the Gordon and Betty Moore Foundation and the NSF MRSEC Program through the Princeton Center for Complex Materials (DMR-0819860).

*xuan.gao@case.edu

[1] D. C. Tsui, H. L. Stormer, and A. C. Gossard, Phys. Rev. Lett. **48**, 1559 (1982).
[2] J. G. Bednorz and K. A. Müller, Z. Phys. B **64**, 189 (1986).
[3] E. Abrahams, P. W. Anderson, D. C. Licciardello, and T. V. Ramakrishnan, Phys. Rev. Lett. **42**, 673 (1979).
[4] S. V. Kravchenko, G. V. Kravchenko, J. E. Furneaux, V. M. Pudalov, and M. D'Iorio, Phys. Rev. B **50**, 8039 (1994).
[5] B. Spivak, S. V. Kravchenko, S. A. Kivelson, and X. P. A. Gao, Rev. Mod. Phys. **82**, 1743 (2010).
[6] E. Abrahams, S. V. Kravchenko, and M. P. Sarachik, Rev. Mod. Phys. **73**, 251 (2001).
[7] Y. Hanein, N. Nenadovic, D. Shahar, H. Shtrikman, J. Yoon, C. C. Li, and D. C. Tsui, Nature (London) **400**, 735 (1999).
[8] S. C. Dultz and H. W. Jiang, Phys. Rev. Lett. **84**, 4689 (2000).
[9] H. W Jiang, C. E. Johnson, K. L. Wang, and S. T. Hannahs, Phys. Rev. Lett. **71**, 1439 (1993).
[10] R. L. Willett, H. L. Stormer, D. C. Tsui, L. N. Pfeiffer, K. W. West, and K. W. Baldwin, Phys. Rev. B **38**, 7881 (1988).
[11] V. J. Goldman, M. Santos, M. Shayegan, and J. E. Cunningham, Phys. Rev. Lett. **65**, 2189 (1990).
[12] H. W. Jiang, R. L. Willett, H. L. Stormer, D. C. Tsui, L. N. Pfeiffer, and K. W. West, Phys. Rev. Lett. **65**, 633 (1990).
[13] H. W. Jiang, H. L. Stormer, D. C. Tsui, L. N. Pfeiffer, and K. W. West, Phys. Rev. B **44**, 8107 (1991).
[14] M. B. Santos, Y. W. Suen, M. Shayegan, Y. P. Li, L. W. Engel, and D. C. Tsui, Phys. Rev. Lett. **68**, 1188 (1992).
[15] Y. P. Li, T. Sajoto, L. W. Engel, D. C. Tsui, and M. Shayegan, Phys. Rev. Lett. **67**, 1630 (1991).
[16] See *Perspectives in Quantum Hall Effects*, edited by S. Das Sarma and A. Pinczuk (John Wiley & Sons, New York, 1997).
[17] G. A. Csáthy, Hwayong Noh, D. C. Tsui, L. N. Pfeiffer, and K. W. West, Phys. Rev. Lett. **94**, 226802 (2005).
[18] B. A. Piot, Z. Jiang, C. R. Dean, L. W. Engel, G. Gervais, L. N.Pfeiffer, and K. W. West, Nature Phys. **4**, 936 (2008).
[19] F. I. B. Williams, P. A. Wright, R. G. Clark, E. Y. Andrei, G. Deville, D. C. Glattli, O. Probst, B. Etienne, C. Dorin, C. T. Foxon, and J. J. Harris, Phys. Rev. Lett. **66**, 3285 (1991).
[20] P. D. Ye, L. W. Engel, D. C. Tsui, R. M. Lewis, L. N. Pfeiffer, and K. West, Phys. Rev. Lett. **89**, 176802 (2002).
[21] Y. P. Chen, R. M. Lewis, L. W. Engel, D. C. Tsui, P. D. Ye, Z. H. Wang, L. N. Pfeiffer, and K. W. West, Phys. Rev. Lett. **93**, 206805 (2004).
[22] H. Zhu, Y. P. Chen, P. Jiang, L. W. Engel, D. C. Tsui, L. N. Pfeiffer, and K. W. West, Phys. Rev. Lett. **105**, 126803 (2010).
[23] B. Tanatar and D. M. Ceperley, Phys. Rev. B **39**, 5005 (1989).
[24] P. M. Platzman, in *The Physics of the Two-Dimensional Electron Gas*, edited by J. T. Devreese and F. M. Peeters (Plenum, New York, 1987).
[25] R. Price, P. M. Platzman, and S. He, Phys. Rev. Lett. **70**, 339 (1993).
[26] (a) X. Zhu and S. G. Louie, Phys. Rev. Lett. **70**, 335 (1993); (b) Phys. Rev. B **52**, 5863 (1995).
[27] K. Yang, F. D. M. Haldane, and E. H. Rezayi, Phys. Rev. B **64**, 081301 (2001).
[28] N. D. Drummond and R. J. Needs, Phys. Rev. Lett. **102**, 126402 (2009).
[29] R. Narevich, G. Murthy, and H. A. Fertig, Phys. Rev. B **64**, 245326 (2001).
[30] R. Chitra, T. Giamarchi, and P. Le Doussal, Phys. Rev. B **65**, 035312 (2001).
[31] X. P. A. Gao, A. P. Mills, Jr., A. P. Ramirez, L. N. Pfeiffer, and K. W. West, Phys. Rev. Lett. **88**, 166803 (2002).
[32] X. P. A. Gao, A. P. Mills, Jr., A. P. Ramirez, L. N. Pfeiffer, and K. W. West, Phys. Rev. Lett. **89**, 016801 (2002).
[33] X. P. A. Gao, G. S. Boebinger, A. P. Mills, Jr., A. P. Ramirez, L. N. Pfeiffer, and K. W. West, Phys. Rev. B **73**, 241315(R) (2006).
[34] R. L. J. Qiu, X. P. A. Gao, L. N. Pfeiffer, and K. W. West, Phys. Rev. B **83**, 193301 (2011).
[35] X. P. A. Gao, G. S. Boebinger, A. P. Mills, Jr., A. P. Ramirez, L. N. Pfeiffer, and K. W. West, Phys. Rev. Lett. **94**, 086402 (2005).
[36] X. P. A. Gao, G. S. Boebinger, A. P. Mills, Jr., A. P. Ramirez, L. N. Pfeiffer, and K. W. West, Phys. Rev. Lett. **93**, 256402 (2004).
[37] Frequently cited effective hole mass in GaAs is $m^* = 0.35m_e$ [H. L. Stormer and W. T. Tsang, Appl. Phys. Lett. **36**, 685 (1980)]. Cyclotron resonance experiments on 10 nm wide GaAs QWs with higher density than our sample gave $m^* = 0.19m_e$ [W. Pan, K. Lai, S. P. Bayrakci, N. P. Ong, D. C. Tsui, L. N. Pfeiffer, and K. W. West, Appl. Phys. Lett. **83**, 3519 (2003)]. By fitting the T-dependent SdH amplitudes to the Lifshitz-Kosevich formula, we estimate $m^* \approx 0.3m_e$ for our low-density 2D hole sample.
[38] A. R. Hamilton, M. Y. Simmons, M. Pepper, E. H. Linfield, P. D. Rose, and D. A. Ritchie, Phys. Rev. Lett. **82**, 1542 (1999).
[39] B. Spivak and S. A. Kivelson, Ann. Phys. (N.Y.) **321**, 2071 (2006).
[40] I. Yang, W. Kang, S. T. Hannahs, L. N. Pfeiffer, and K. W. West, Phys. Rev. B **68**, 121302 (2003).
[41] S. Chakravarty, S. Kivelson, C. Nayak, and K. Voelker, Philos. Mag. B **79**, 859 (1999).